

Reduced Dark Counts in Optimized Geometries for Superconducting Nanowire Single photon Detectors

Mohsen K. Akhlaghi,^{1, a)} Haig Atikian,² Amin Eftekharian,^{1,3} Marko Loncar,² and A. Hamed Majedi^{1,3,2, b)}

¹⁾*ECE Department, University of Waterloo, 200 University Ave West, Waterloo, ON, Canada, N2L 3G1*

²⁾*School of Engineering and Applied Sciences, Harvard University, Cambridge, MA 02138*

³⁾*Institute for Quantum Computing, University of Waterloo, 200 University Ave West, Waterloo, ON, Canada, N2L 3G1*

(Dated: 24 October 2018)

We have experimentally compared the critical current, dark count rate and photo-response of 100nm wide superconducting nanowires with different bend designs. Enhanced critical current for nanowires with optimally rounded bends, and thus with no current crowding, are observed. Furthermore, we find that the optimally designed bend significantly reduces the dark counts without compromising the photo-response of the device. The results can lead to major improvements in superconducting nanowire single photon detectors.

Single photon detectors are essential components in diverse fields including quantum optics and information¹, quantum key distribution², lunar laser communication³, diagnosis of integrated circuits⁴ and characterization of single photon sources⁵. Superconducting nanowire single photon detectors (SNSPDs) outperform other detectors in merits such as infrared quantum efficiency, dark count rate, timing jitter⁶, and maximum count rate⁷. Thus, they are considered as a promising technology for demanding photon counting applications⁸.

SNSPDs are typically made of current biased meandering superconducting nanostrips (usually ~ 100 nm wide) with 180-degree turns. The photons are focused on the parallel nanostrips that form the active area, while the turns only serve the purpose of electrical connection. The closer the bias current is to the critical current of the nanostrips, the higher the detection efficiency, but also the higher the dark count rate⁸. Although the turns are typically placed outside the photon absorbing area, and thus do not directly contribute to the photon detection, they can degrade the overall performance of the detector by acting as current bottlenecks or by generating dark counts.

Recently, Clem et al.⁹ recapped the possible impact of sharp turns on SNSPDs: the current crowds at the inner edge thus reducing the measured critical current of the meander. Also, the current bottleneck in wide superconducting strips (300nm to $1\mu\text{m}$ wide) with sharp bends has been experimentally demonstrated^{10,11}. However, an open question remains on the impact of current crowding on present SNSPDs that feature much narrower strips (~ 100 nm wide), in which both increased ratio of the bend curvature (due to inherent finite fabrication resolution) to nanowire width, and reduced width to coherence length ratio make the expected effect smaller^{9,11}. Here we present experiments that probe the current crowding

effect on the critical current of superconducting nanostrips with a width comparable to the commonly used width in modern SNSPDs. We also report on the effect of sharp bends on the observed photo-response and dark counts.

A typical device presented in this letter is illustrated in Fig. 1(a). A nanowire, 100nm wide and 8nm thick, is bent either 90-degree or 180-degree, and connected to large pads (not shown) by a gradual transition to wider strips. The nanowire length is $\sim 0.5\mu\text{m}$ on either side of the bend. Our bends fall into two categories: optimally designed with no current crowding and thus no expected critical current reduction, and traditional bends made without optimal considerations.

Figure 1(b) shows an example of our optimum bends. To find the optimal bend design, we numerically solve $\nabla \cdot \mathbf{K} = 0$ and $\nabla \times \mathbf{K} = -d/\lambda^2 \mathbf{H} \approx 0$ within the area enclosed by the white lines⁹, where \mathbf{K} is the sheet current density, d is the nanowire thickness and λ is the magnetic penetration depth. The boundary conditions are $\mathbf{n} \cdot \mathbf{K}_l = 0$, and $\mathbf{n} \times \mathbf{K}_i = 0$, where \mathbf{n} is a vector normal to the edge, \mathbf{K}_l is \mathbf{K} on the lateral boundaries (solid white lines) and \mathbf{K}_i is \mathbf{K} on the input boundaries (dotted white lines). Next, we find the streamlines of the vector field \mathbf{K} (dashed blue and red lines). Any two streamlines (dashed red lines) that enclose a surface within which $|\mathbf{K}|$ remains less than or equal to $|\mathbf{K}_i|$, form an optimized bend (because \mathbf{K} within them satisfies the same above boundary value problem, and $|\mathbf{K}|$ in the bend does not exceed $|\mathbf{K}|$ within the nanowire).

Four different 90-degree bends have been investigated: (i) optimized bend with the smallest possible footprint, (ii) optimized bend twice as big as the smallest one (to make it more tolerant to fabrication errors), (iii) sharp bend and (iv) 45° bend (as a structure between worse and best case scenarios) (see Figs. 1(b) through 1(e)). The smallest possible optimum 180-degree turn (200nm spacing) is shown in Fig. 1(f). It will be compared with a sharp 180-degree turn (200nm spacing) and a bigger optimum turn (300nm spacing) as shown in Figs. 1(g) and

^{a)}mkesava@maxwell.uwaterloo.ca

^{b)}ahmajedi@maxwell.uwaterloo.ca

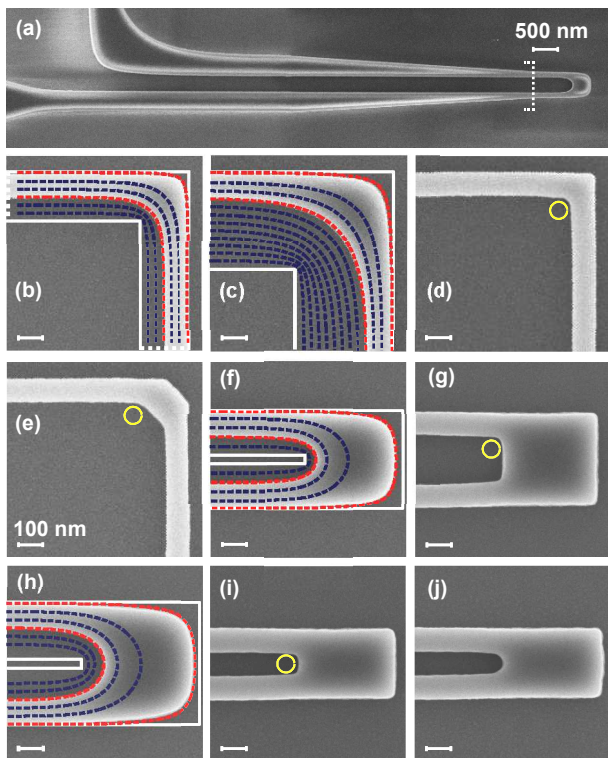


FIG. 1. (Color online) Scanning electron microscope images of the nanowires explored in this letter. (a) A typical nanowire structure examined in this letter and its connection lines. (b) and (c) two optimized 90-degree bends. (d) and (e) sharp and 45° 90-degree bends. (f) and (g) optimized and sharp 180-degree turns with 200nm spacing. (h) optimized 180-degree turn with 300nm spacing. (i) and (j) sharp and circular (radius = 50nm) 180-degree turns with 100nm spacing. The circles are eye guides with 35nm radius. Blue and red dashed lines are current streamlines calculated for a superconductor thin film enclosed by solid white lines. All the parts, except (a) share the same length scale.

1(h). Finally, Figs. 1(i) and 1(j) present a commonly used bend in present SNSPDs (sharp bend with 100nm spacing) and the same but circularly rounded (radius = 50nm).

The devices are made of 8nm thick NbTiN films deposited on oxidized silicon. Hydrogen silsesquioxane resist was spin-coated on top and patterned using 125keV electron-beam lithography. The write parameters were carefully tuned to achieve nanostructures as identical as possible to the designed curvatures (see red dashed lines in Fig. 1 overlaid on the nanowire images). The resist was developed in a tetra-methyl ammonium hydroxide solution, and the pattern was transferred into the film using ion beam milling with Argon gas. The critical temperature of the film before and after nano-patterning was measured to be 8.4K

The critical current, dark count and photo response of a nanowire is a function of its dimensions (thickness and width), as well as superconducting thin film quality.

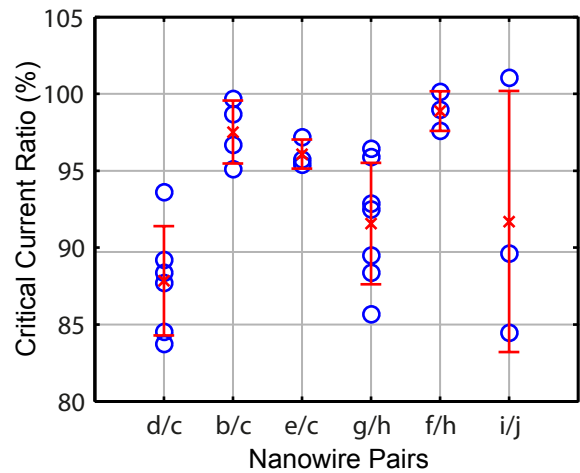


FIG. 2. (Color online) I_c^α/I_c^β for closely fabricated bent nanowire pairs labeled by α/β , where α and β correspond to the insets of Fig 1. The red error bars indicate the mean and standard deviation for measurements on each pair.

Therefore, when investigating the effect of bend design, it is essential to keep the nanowires identical except at the bend. In our experiments, we only juxtapose two different bends from the designs in Fig. 1 that satisfy the following conditions: (i) both are either 90-degree or 180-degree, and (ii) both are fabricated few μm apart on the same chip. The first condition keeps the two geometries as similar as possible and therefore minimizes slight width changes when different geometries are exposed by the electron-beam. The second condition assures the two nanowires share the most identical film thickness/quality as well as equivalent fabrication processing (to make effects of many factors including resist variations, proximity dose effects, and others less significant).

Each pair of nanowires has a common electrical ground. Each of the other terminals connect to a 490nH inductor (placed next to the chip) and then to a room temperature bias-T by a coax cable (50 Ω impedance). A computer controlled voltage source that measures its output current (Keithley 2400) is connected to the DC port of the bias-T via a low-pass filter (to reduce high frequency noise and interference). The high frequency response of the nanowire (after room temperature amplification) is monitored through the RF port on an oscilloscope or a programmable counter. A single mode fiber, placed several centimeters away from the chip uniformly radiates the pair with 1310nm photons from an attenuated pulsed laser source (width \sim 200ps, repetition rate 20MHz). The 50 Ω impedance together with the inductor make a large enough time constant to observe relaxation oscillations in all our current-voltage curve measurements, thus ensuring the peak current is the (experimental) critical current¹². The measurements have been done by installing the samples in a dipstick probe and immersing it in liquid Helium (monitored temperature \sim 4.2K).

Figure 2 summarizes the critical current measurements of the samples. The horizontal axis (i.e. α/β) specifies a pair of nanowires using the characters that name the bends in the insets of Fig. 1. The blue circles show the ratio of the critical currents of the nanowires within the same pair (i.e. I_c^α/I_c^β). The red crosses indicate the mean and the bars show the standard deviation for measurements of each pair type. The pairs d/c and g/h show the sharpest bends have considerably lower critical currents compared to the bigger optimum bends (see the means). The pairs b/c and f/h show while both of the smallest and bigger optimum bends work appropriately, bigger bends still slightly improve the critical current. We attribute this observation to smaller current density at the inner edge of the bigger designs and therefore their improved tolerance to fabrication errors. The pair e/c shows the moderate performance of 45° 90-degree bends. Finally i/j shows while there is no optimum design for a 180-degree turnaround of 100nm wide strips spaced by 100nm, cir-

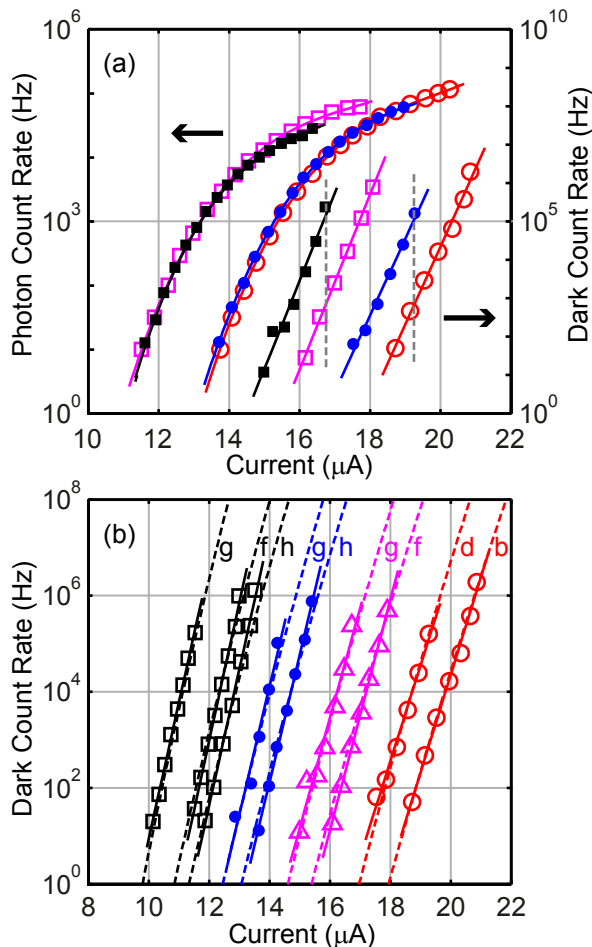


FIG. 3. (Color online) (a) Photo-response and dark count measurements for samples of pairs d/b and g/f. (b) Dark count measurements for more samples. Each symbol is for devices on the same chip. The letters refer to insets of Fig. 1. All the lines are for eye guide.

cularly rounded bends can improve the reduced critical current by a considerable factor. We have also confirmed satisfactory operation of our measurement setup by measuring the critical current of our devices several times and finding negligible mean normalized error (equal to $\sim 0.4\%$).

The error bars of Fig. 2 show large variations for different samples of the same pair. An approximate trend is that the sharper the bend the larger the variation. We attribute this to the uncontrollability of the radius of curvature ($\sim 35\text{nm}$, see yellow circles of Fig. 1) for sharp bends. For the pair i/j the variation is maximum because $\sim 35\text{nm}$ could almost change device i to j. This can be a possible explanation for small fabrication yield of SNSPDs⁸ where the large number of serially connected 180-degree turns in a meander makes having at least one very sharp bend quite possible.

We have also measured the dark counts and photon counts generated by the nanowires of a given pair. The room temperature end of the fiber was blocked by a shutter for dark count vs bias current measurements. Photon counts are measured by exciting the pairs with weak laser pulses and subtracting the expected dark counts at the same bias. We ensure single photon sensitivity by checking the linear proportionality of the photon counts with the number of incident photons¹³.

Figure 3(a) shows the result for two of our pairs d/b (circles) and g/f (squares). The sharper bends are shown by filled symbols. The photo-response of the bends that make a pair is almost similar for their common range of bias. This is expected as the devices in a given pair are identical except at the small bending area. However, at the same bias current, and therefore at the same quantum efficiency, utilizing an optimum bend can reduce the dark count rate by orders of magnitude, a significant result for SNSPDs. We also note that the optimum bends further increase the range of bias and thus enable operating at higher quantum efficiency (or longer wavelength).

Illustrated in Fig. 3(b) are dark count measurements for some of the nanowires fabricated on different chips (each symbol is for devices on the same chip). About $\pm 20\%$ variations for critical current measurements of our optimum bends can be seen. Investigating the devices under scanning electron microscope, we have not observed significant dimension changes. Therefore, we attribute this variations to slight film thickness/quality change from chip to chip. However, on each chip the trend is the same: the sharper the bend the smaller the critical current, and the higher the dark counts.

At the inner edge of a sharp 90-degree turn with radius of curvature equal to $\sim 35\text{nm}$, we calculate the density of the sheet current, $|\mathbf{K}|$, ~ 1.7 times higher than the same density for an optimized bend (smallest possible footprint). So, a vortex at the edge of a sharp turn faces almost the same barrier as a vortex at the edge of an optimum bend but at a bias current ~ 1.7 times smaller (neglecting radius of curvature effects⁹ which is reasonable because $\sim 35\text{nm}$ is bigger than the coherence length).

Therefore, assuming vortices overcoming an edge barrier is the origin of dark counts¹⁴, we expect having the dark count vs bias current of a sharp turn to be approximately shifted to smaller currents by $\sim 1/1.7$. However, in none of our nanowires have we observed such a large shift. The trend of disagreement with this theory is nevertheless the same as what has been observed for critical current measurements on wider strips^{10,11}.

To conclude, we have explored the possible adverse impact of sharp turns on SNSPDs through (i) limiting their bias current and thus limiting their quantum efficiency, and (ii) generating excess dark counts not generated by straight nanowire segments where photons are detected. We expect the utilization of optimally designed bends to further push SNSPDs to more efficient single photon detection at longer wavelengths while generating less dark counts.

ACKNOWLEDGMENTS

We acknowledge the financial support of OCE, NSERC and IQC. The authors would like to acknowledge Robin Cantor for helpful comments. This work was performed in part at the Center for Nanoscale Systems (CNS), a member of the National Nanotechnology Infrastructure Network (NNIN), which is supported by the National Science Foundation under NSF award no. ECS-0335765. CNS is part of Harvard University.

- ¹E. Knill, R. Laflamme, and G. J. Milburn, *Nature* **409**, 46–52 (2001).
- ²H. Takesue, S. W. Nam, Q. Zhang, R. H. Hadfield, T. Honjo, K. Tamaki, and Y. Yamamoto, *Nature Photon.* **1**, 343–348 (2007).
- ³M. E. Grein, A. J. Kerman, E. A. Dauler, O. Shatrovov, R. J. Molnar, D. Rosenberg, J. Yoon, C. E. Devoe, D. V. Murphy, B. S. Robinson, and D. M. Boroson, 2011 International Conference on Space Optical Systems and Applications, ICSOS'11, 78–82 (2011).
- ⁴J. Zhang, N. Boiadjieva, G. Chulkova, H. Deslandes, G. N. Gol'tsman, A. Korneev, P. Kouminov, M. Leibowitz, W. Lo, R. Malinsky, O. Okunev, A. Pearlman, W. Slysz, K. Smirnov, C. Tsao, A. Verevkin, B. Voronov, K. Wilsher, and R. Sobolewski, *Electron. Lett.* **39**, 1086–1088 (2003).
- ⁵M. J. Stevens, R. H. Hadfield, R. E. Schwall, S. W. Nam, R. P. Mirin, and J. A. Gupta, *Appl. Phys. Lett.* **89** (2006).
- ⁶R. H. Hadfield, *Nature Photonics* **3**, 696–705 (2009).
- ⁷M. K. Akhlaghi and A. H. Majedi, *Opt. Express* **20**, 1608–1616 (2012).
- ⁸C. M. Natarajan, M. G. Tanner, and R. H. Hadfield, *Superconductor Science and Technology* **25**, 063001 (2012).
- ⁹J. R. Clem and K. K. Berggren, *Phys. Rev. B* **84**, 174510 (2011).
- ¹⁰H. L. Hortensius, E. F. C. Driessen, T. M. Klapwijk, K. K. Berggren, and J. R. Clem, *Applied Physics Letters* **100**, 182602 (2012).
- ¹¹D. Henrich, P. Reichensperger, M. Hofherr, K. Ilin, M. Siegel, A. Semenov, A. Zotova, and D. Y. Vodolazov, arXiv:1204.0616v1 (unpublished).
- ¹²A. J. Kerman, J. K. W. Yang, R. J. Molnar, E. A. Dauler, and K. K. Berggren, *Phys. Rev. B* **79** (2009).
- ¹³M. K. Akhlaghi, A. H. Majedi, and J. S. Lundeen, *Opt. Express* **19**, 21305–21312 (2011).
- ¹⁴L. N. Bulaevskii, M. J. Graf, C. D. Batista, and V. G. Kogan, *Phys. Rev. B* **83**, 144526 (2011).